QUANTUM NATURE OF ELECTRONS IN CLASSICAL X-RAY FELS*

Petr M. Anisimov#, LANL, Los Alamos, NM 87545, USA

Abstract

An x-ray free electron laser (FEL) is considered by many to be a completely classical device. Yet, some have investigated operating regimes where the underlying physics transitions from a classical to a quantum description. Focusing on the collective behaviour of electrons, they have introduced symmetrized bunching operators and have found an additional energy spread due to recoil, mediated through a quantum FEL parameter.

This work focuses on the quantum nature of a single electron, which is best described, not by a point particle, but by a wave packet. Owing to free space dispersion, one can define the smallest-sized wave packet at an FEL entrance that remains as such throughout an FEL. By utilizing this packet size, we have developed a 1D FEL theory that includes how quantum effects affect bunching.

The smallest-sized wave packet is related to the quantum FEL parameter and offers new insights into the classical-to-quantum transition. It can be generalized to include 3D effects and offers a convenient way to classify FELs. Our theory indicates that gain reduction due to quantum averaging is much stronger than previously believed and will significantly affect harmonic lasing in x-ray FELs (XFELs).

INTRODUCTION

Interest in XFELs has grown in response to the expanding scientific demand in coherent x-ray light sources. XFELs, such as the LCLS at SLAC (USA) [1] and SACLA at Spring-8 (Japan) [2], deliver ultra-bright X-ray pulses having femtosecond duration. Their peak brilliance is about eight orders of magnitude higher than that from most other X-ray sources. The combination of high pulse energy and femtosecond pulse duration of coherent XFEL pulses has created new fields of research in ultrafast chemistry, structural biology and coherent diffractive imaging [3].

The FEL was invented by John Madey [4] who used a quantum mechanical description to arrive at a classical result for the low-gain lasing regime. Thus, the FEL is considered by many to be a completely classical device [5-7]. However, there has been a significant effort to formulate a quantum mechanical description for FELs [8-12] even though XFELs built to date are well described by the classical theory (as their bandwidth is much larger than the recoil frequency) [13].

The quantum regime for FEL operation discussed in Ref. [13] was further investigated in Refs. [14-19]. It was shown that the classical-to-quantum transition is controlled by a "quantum FEL parameter", defined as the ratio between the FEL bandwidth and the photon recoil energy [20]. The quantum regime of operation requires the quantum FEL parameter to be small, a regime that cannot be reached by existing XFELs [1, 2].

Future XFELs are now being designed in response to demand for ever shorter radiation wavelengths and narrower bandwidths. However, cost limitations for future facilities drives their design to utilize accelerators with as low a beam energy as possible. These opposing design criteria exacerbate quantum mechanical effects requiring careful consideration of their impact on lasing performance.

Here we focus on the quantum nature of a single electron and determine how it affects classical XFEL performance. Starting with the classical 1D theory and an analysis of the free space dispersion of an electron wave packet, we construct a hybrid 1D FEL theory that accounts for quantum uncertainty of the electron position inside an XFEL. This theory facilitates a unified description of XFELs and indicates that the planned MaRIE XFEL at Los Alamos National Lab [21] will be affected.

CLASSICAL 1D THEORY

XFELs are lasers that use relativistic electrons moving freely through a periodic magnetic structure in order to generate radiation. The magnetic structure, an undulator, is characterized by wiggle period λ_u and strength parameter $K = eB_0/k_u mc$, where B_0 is a peak magnetic field and $k_u = 2\pi/\lambda_u$. In a planar undulator, electrons with energy γ_0 in mc^2 units generate x-ray radiation at a wavelength $\lambda = \frac{\lambda_u}{2\gamma_0^2}\left(1+K^2/2\right)$.

The fundamentals of FEL instability are captured by the 1D theory with universal scaling in terms of the FEL parameter $\rho = \frac{1}{2\gamma_0}\sqrt[3]{\frac{I}{I_A}\frac{\lambda_u^2 K^2 JJ_1}{8\pi A}}$ for an electron beam with the peak current I and the transverse area A. Here I_A =17 kA is the Alfven current and $JJ_n = J_{\lfloor n/2\rfloor}(nY) + J_{\lfloor n/2\rfloor+1}(nY)$ with $Y = -K^2/(4+2K^2)$ is the energy exchange parameter. The independent variable is the distance along the undulator, $z = \bar{v}_z t/L_{g0}$, measured in the units of the 1D gain length $L_{g0} = \lambda_u/4\pi\rho$; and the α^{th} electron is described by its ponderomotive phase with respect to the radiation, $\theta_\alpha = (k+k_u)\bar{v}_z t - kct$, and the relative energy detuning, $\eta_\alpha = (\gamma-\gamma_0)/\rho\gamma_0$. The complete set of coupled first-order differential equations has the following form:

*Work supported by the U.S. Department of Energy through the LANL/LDRD Program. LA-UR–15– 26403
#petr@lanl.gov

ISBN 978-3-95450-134-2

$$\frac{d\theta_\alpha}{dz} = \eta_\alpha \tag{1}$$

$$\frac{d\eta_\alpha}{dz} = -2\,\mathrm{Re}\left(Ee^{i\theta_\alpha}\right) \tag{2}$$

$$\frac{dE}{dz} = \frac{1}{N}\sum_{\alpha=1}^{N} e^{-i\theta_\alpha} \tag{3}$$

where the radiation field, E, is normalized to the field at saturation $E_{sat} = \frac{\mu_0 cKJJ_1}{2\gamma_0}\frac{I}{A}L_{g0}$.

Equations (1) and (2) are the pendulum equations and describe the motion of an electron in the ponderomotive potential created by the x-ray radiation. There are two classes of electrons – trapped (in the well) and untrapped. Trapped electrons bunch together and emit coherent radiation according to Eq. (3), which in turn deepens the ponderomotive well. This captures a fraction of the untrapped electrons and provides additional energy for further increasing x-ray radiation and trapping efficiency. Once all electrons are trapped at about $z_{\mathrm{sat}} = 10$, the saturation is reached.

We analyse the growth of FEL instability using the Vlasov equation for an ensemble of electrons with the distribution, $F_0(\eta) = 1/(2\Delta)$ for $|\eta - \delta| \le \Delta$ [5] and show that the x-ray radiation field obeys the equation:

$$\frac{dE^3}{dz^3} + 2i\Delta\frac{dE^2}{dz^2} - \left(\delta^2 - \Delta^2\right)\frac{dE}{dz} - iE = 0$$

Looking for a solution of the form $E = E_0 e^{-i\delta z + i\lambda z}$, one obtains the cubic characteristic equation:

$$(\lambda - \delta)\left(\lambda^2 - \Delta^2\right) + 1 = 0 \tag{4}$$

where the growth rate for the FEL instability is given by the negative imaginary part of a complex root (see Figure 1).

QUANTUM ELECTRON

Classical FEL theory depends on the localization of an electron in its ponderomotive well. According to quantum mechanics, an electron is not a point particle and therefore must be treated as a wave packet:

$$\psi(s,z) = e^{ik_0(s-z)}\frac{e^{-(s-z)^2/4\Delta s(z)^2}}{\sqrt{\sqrt{2\pi}\Delta s(z)}}$$

having energy $\gamma_0 = \sqrt{1 + \hbar^2 k_0^2/m_0^2c^2}$ in mc^2 units. Consequently, electrons can only be localized in the ponderomotive well to no better than $2\Delta s/\lambda$ and the ponderomotive phase of the α^{th} electron is distributed as:

$$W_\alpha(\theta,z) = \frac{e^{-(\theta-\theta_\alpha)^2/2\sigma(z)^2}}{\sqrt{2\pi}\sigma(z)}$$

with $\sigma(z) = 2\pi\Delta s(z)/\lambda$.

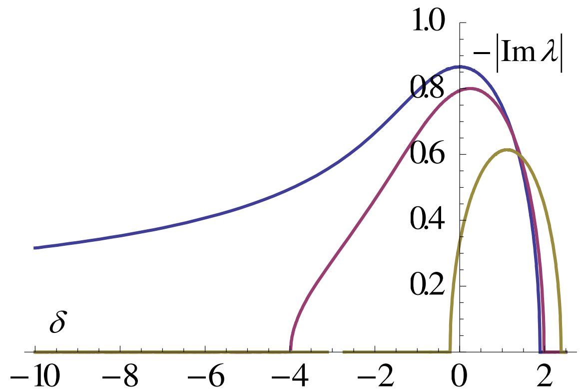

Figure 1: Growth rate for different energy spreads: $\Delta = 0$ (blue), $\Delta = 1/2$ (red), $\Delta = 1/0.8$ (yellow).

Owing to free space dispersion, the size of the wave packet cannot be infinitely small. Starting with a width Δs_0, it grows according to

$$\Delta s^2(z) = \Delta s_0^2 + \frac{d_z^2 L_{g0}^2}{\bar{v}_z^2 \Delta s_0^2} z^2$$

where $\bar{v}_z = c\beta\left(1 - K^2/4\gamma_0^2\right)$ is the average electron longitudinal velocity in an undulator and $d_z = \frac{\lambda_c c}{4\pi\gamma_0^3}\left(1 + \frac{K^2}{2}\right)$ is the free space dispersion modified by the presence of the undulator field. Thus, the initial size of the wave packet, Δs_0, that minimizes the spreading of the wave packet inside an undulator of the dimensionless length, L, is $\Delta s_0^2 = d_z L_{g0} L/\bar{v}_z$.

The quantum mechanical nature of electron limits the smallest-sized wave packet at the end of an undulator to $\Delta s_f^2 \approx \frac{\lambda_c L_{g0} L}{2\pi\gamma_0^3}\left(1 + \frac{K^2}{2}\right)$, which is 7% of the radiation wavelength for MaRIE parameters [21]! Therefore, modification of the 1D theory is needed to include wave packet spreading in order to properly describe MaRIE XFEL performance.

HYBRID 1D THEORY

The 1D FEL theory can be amended by including wave packet spreading and quantum averaging. The modified set of coupled first-order differential equations takes the following form:

$$\frac{d\theta_\alpha}{dz} = \eta_\alpha$$

$$\frac{d\eta_\alpha}{dz} = -2\sum_n \frac{JJ_n}{JJ_1}\mathrm{Re}\left(E_n\left\langle e^{in\theta}\right\rangle_\alpha\right)$$

$$\frac{dE_n}{dz} = \frac{JJ_n}{JJ_1}\frac{1}{N}\sum_{\alpha=1}^{N}\left\langle e^{-in\theta}\right\rangle_\alpha$$

$$\frac{d\sigma^2}{dz} = \frac{1}{2\bar{\rho}^2\sigma_0^2} z$$

ISBN 978-3-95450-134-2

where the quantum averaging is $\left\langle e^{in\theta}\right\rangle_\alpha = e^{-n^2\sigma^2/2}e^{in\theta_\alpha}$, the quantum FEL parameter is $\bar{\rho} = \rho(mc\gamma/\hbar k)$, and n is the harmonic lasing number [22-25].

The solution of the last equation is $\sigma(z)^2 = \sigma_0^2 + z^2/4\bar{\rho}^2\sigma_0^2$ and for $z_f = z_{sat}$ the minimal final uncertainty for the ponderomotive phase is $\sigma_f = \sqrt{z_{sat}/\bar{\rho}}$. This smallest-sized electron wave packet depends on the quantum FEL parameter and provides new insights into the classical-to-quantum transition.

In the classical regime, $\bar{\rho} >> 1$ (i.e. $\sigma_f << \pi$) an electron can be treated as a point particle since this smallest-sized wave packet fits easily inside a ponderomotive well. In the intermediate regime, where $\bar{\rho} = 1$ (i.e. $\sigma_f \approx \pi$), an electron extends slightly into neighbouring wells (see Figure 2). Lastly, in the quantum regime where $\bar{\rho} << 1$ (i.e. $\sigma_f >> \pi$), an electron occupies more than a single ponderomotive well. In the particular case where $\bar{\rho} = 0.4$ (see Ref. [16]), the FEL spectrum makes a transition from continuous to discreet, as an electron has a significant probability of being located in multiple nearest-neighbour wells (see Figure 2).

DISCUSSION

Previous theoretical works focused on collective bunching behaviour and used a symmetrized momentum bunching operator for quantization [19]. It has been found that the growth rate equation is similar to that from the dispersion relation for the classical FEL with initial energy spread $\Delta = 1/2\bar{\rho}$ (see Eq. 4). This extra term represents the intrinsic quantum momentum spread due to recoil that, in dimensional units, is given by $\hbar k/2$.

Hybrid 1D FEL theory provides new insight into FEL operation in the quantum regime by relating the smallest-sized wave packet to the size of the ponderomotive well. The wave packet description of an electron also carries an intrinsic quantum momentum spread that, in dimensionless units, has an initial energy spread $\Delta_0 = 1/\sqrt{2z_{sat}\bar{\rho}}$. Here, contrary to expectations, the energy spread tends to zero for a point particle, $\bar{\rho} >> 1$.

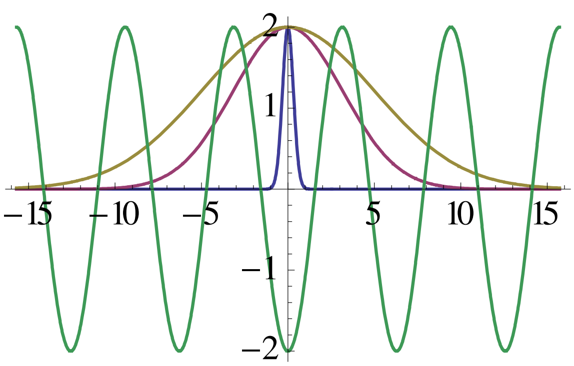

Figure 2: Electron probability distribution at the end of an undulator, $W_\alpha(\theta,\sigma_f)$, in the ponderomotive potential (green) for different values of the quantum FEL parameter: $\bar{\rho} = 100$ (blue), $\bar{\rho} = 1$ (red), and $\bar{\rho} = 0.4$ (yellow).

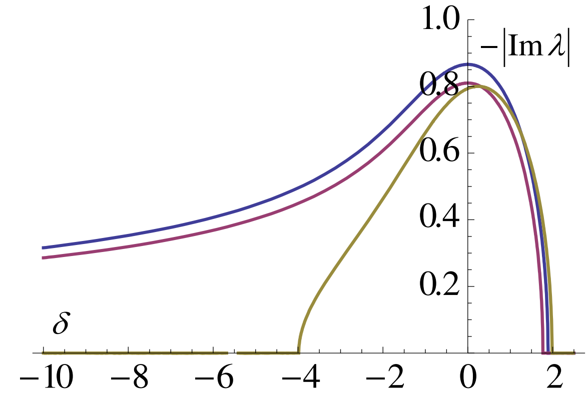

Figure 3: Growth parameter for a mono-energetic beam without quantum averaging (blue) and with quantum averaging for $\bar{\rho} = 50$ (red). The yellow line is for the growth parameter based on Ref. [16] for $\bar{\rho} = 1$.

One can perform a growth rate analysis for 1D hybrid theory by assuming a constant-sized wave packet since the minimum uncertainty wave packet spreads little inside an undulator:

$$\frac{dE_n^3}{dz^3} + 2i\delta\frac{dE_n^2}{dz^2} - \left(\delta^2 - \Delta^2\right)\frac{dE_n}{dz} - q_n^2 iE_n = 0$$

where $q_n = \frac{JJ_n}{JJ_1}e^{-n^2\sigma^2/2}$. Here, we assume single harmonic lasing, where only the n^{th} harmonic is generated and all other harmonics are suppressed [22-25].

The quantum nature of an electron, captured by the 1D hybrid theory, does not introduce energy spread. However, the FEL growth rate is still reduced due to quantum averaging. Figure 3 shows the FEL growth parameter as a function of detuning including reductions of the growth parameter based on quantum averaging and on the theory from Ref. [16]. For example, the on-resonance growth rate for a mono-energetic electron beam is reduced due to quantum averaging by $e^{-n^2\sigma^2/3}$, which is much stronger than one would expect based on the previous analysis.

1D theory does not take into account 3D effects that increase the gain length over L_{g0} and require a longer undulator in order to reach saturation. The quantum FEL parameter does not take into account such effects. The smallest-sized wave packet, on the other hand, becomes larger in size in order to accommodate the longer undulator length and thus behaves more quantum than would be otherwise expected. For a given smallest-sized wave packet with an FEL parameter ρ, there is a family of XFELs which generate x-ray radiation at a given energy that are equally affected by the quantum nature of electrons. Therefore, one can classify the quantum nature of XFELs based on the smallest-sized wave packet.

ISBN 978-3-95450-134-2

Figure 4 shows the x-ray FEL families for different wave packet sizes.

The final point of our discussion concerns harmonic lasing [22-25]. The reduction in performance caused by quantum averaging is stronger here due to the quadratic dependence on the harmonic number. Table 1 shows the expected gain reduction for the 3rd harmonic lasing with suppressed fundamental for current/planned facilities. While the growth rate for the fundamental is reduced by a few percent in a case of MaRIE facility, quantum averaging will reduce the on-resonance growth rate by 60%.

CONCLUSIONS

The quantum nature of an electron expresses itself through its wave nature. The wave packet description of an electron is closer to a classical point particle description than it is to a plane wave description but free space dispersion effects remain. We have amended 1D FEL theory in order to include quantum averaging over the nonlocal electron wave packet. A long wave packet does not spread as much as a short wave packet, but it might still be longer at the end of the undulator. Thus, we have focused on the smallest wave packet that minimizes wave packet spreading at the end of an undulator.

We have showed that classification of quantum FELs can be done based on either the quantum FEL parameter or the minimum uncertainty of wave packet spreading. However, when 3D effects are included, the later approach seems to be preferred over former. Furthermore, our approach provides new insights into the classical to the quantum regime transition.

Based on the information in Table 1, one can estimate σ_f including 3D effects for different FEL facilities. Using the 1D expression for the minimal final uncertainty of the ponderomotive phase, one can define an effective quantum FEL parameter. In the case of the MaRIE facility, $\bar{\rho}_{\text{eff}} = 50$, putting it in the classical domain based on the previous classification. However, its on-resonance growth parameter is reduced by as much as one would expect from the previous treatment with $\bar{\rho} = 1$.

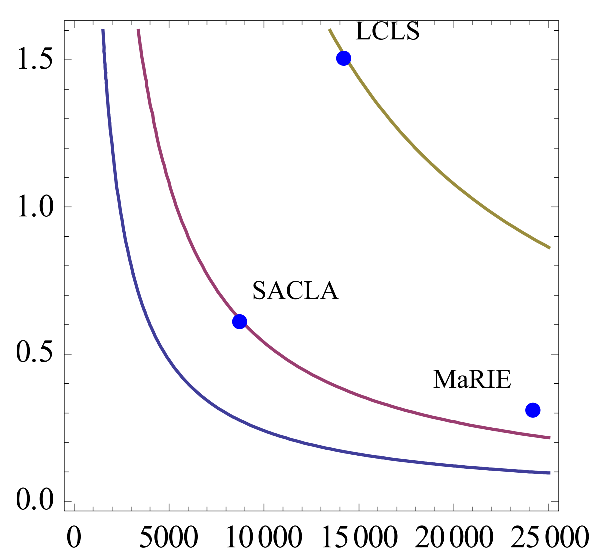

Figure 4: X-ray FEL families for $\sigma_f = 0.45$ (blue), $\sigma_f = 0.30$ (red), and $\sigma_f = 0.15$ (yellow) for $\rho = 5\times10^{-4}$. The vertical axis is in Angstrom and the horizontal axis is the energy of electrons in mc^2 units.

Table 1: Gain Reduction Comparison for Various Facilities

XFEL	**Energy**	λ_r	$2\Delta s_f/\lambda_r$	Γ_{qu}/Γ_{3rd}
LCLS	14 GeV	1.5A	5%	0.93
European	17.5 GeV	0.5A	8%	0.82
PAL	10 GeV	0.6A	10%	0.75
SACLA	8.5 GeV	0.6A	12%	0.64
MaRIE	12 GeV	0.3A	14%	0.58

REFERENCES

[1] P. Emma, et al., Nat. Photonics 4 (2010) 641.
[2] T. Ishikawa et al., Nat Photonics 6 (2012) 540.
[3] M. Yabashi, H. Tanaka, and T. Ishikawa, J. Synch. Rad. 22 (2015) 477.
[4] J.M.J Madey, J. Appl. Phys. 42 (1971) 1906.
[5] P. Schmuser, et al., "Free-Electron Lasers in the Ultraviolet and X-ray Regime," (Springer Tracts in Modern Physics 2014).
[6] E.L. Saldin, E.A. Schneidmiller, and M.V. Yurkov, "The Physics of Free Electron Lasers," (Springer, Berlin Heidelberg 2000).
[7] H.P. Freund and T.M. Antonsen, "Principles of Free-Electron Lasers," (Chapman & Hall, London, 1996).
[8] W. Becker and M.S. Zubairy, Phys. Rev. A 25 (1982) 2200.
[9] W. Becker and J.K. McIver, Phys. Rev. A 27 (1983) 1030.
[10] R. Bonifacio and F. Casagrande, Optics Comm. 50 (1984) 251
[11] R. Bonifacio, C. Pellegrini and L. Narducci, Opt. Commun. 50 (1984) 373.
[12] G. Preparata, Phys. Rev. A 38 (1988) 233.
[13] I.V. Smetanin, Laser Physics 7 (1997) 318.
[14] R. Bonifacio, et al., Europhys. Lett. 69 (2005) 55.
[15] R. Bonifacio, N. Piovella and G.R.M. Robb, Nucl. Instrum. and Meth. in Phys. Res. A 543 (2005) 645.
[16] R. Bonifacio, et al., Phys. Rev. ST Accel. Beams 9 (2006) 090701.
[17] R. Bonifacio, et al., Opt. Commun. 274 (2007) 347.
[18] N. Piovella, et al., Phys. Rev. Lett 100 (2008) 044801.
[19] C.B. Schroeder, C. Pellegrini and P. Chen, Phys. Rev. E 64 (2001) 056502.
[20] R. Bonifacion and F. Casagrande, Nucl. Inst. and Meth. A 237 (1985) 168.
[21] B.E. Carlsten et al., in Proceedings of the Particle Accelerator Conference 2011, Paper TUODS1.
[22] B.W.J. McNeil, et al., Phys. Rev. Lett. 96 (2006) 084801.
[22] E.A. Schneidmiller and M.V. Yurkov, Phys. Rev. ST Accel. Beams 15 (2012) 080702.
[24] H.P. Freund, Phys. Rev. ST Accel. Beams 17 (2014) 010702.
[25] G. Penn, Phys. Rev. ST Accel. Beams 18 (2015) 060703.

ISBN 978-3-95450-134-2